DRÆM – A discriminatively trained reconstruction embedding for surface anomaly detection

Supplementary material

Vitjan Zavrtanik Matej Kristan Danijel Skočaj
University of Ljubljana, Faculty of Computer and Information Science
{vitjan.zavrtanik, matej.kristan, danijel.skocaj}@fri.uni-lj.si

1. MVTec qualitative examples

Figures 1,2 and 3 show qualitative examples for each individual class of the MVTec anomaly detection dataset [1]. The qualitative comparison of DRÆM to the recent US [2] and RIAD [7] methods is shown in Figure 4. In Figure 5 the detection ability of DRÆM on various atypical anomalous images is shown. The images in Figures 1, 2, 3, 4 and 5 are best viewed zoomed in.

2. DAGM qualitative examples

Figures 6 and 7 show qualitative examples for each class of the DAGM dataset [6]. The anomaly maps generated by the method by Božič *et al*. [3] are shown in addition to the DRÆM anomaly maps for comparison and to demonstrate the high accuracy localization ability of DRÆM. Due to the small size of anomalies, the images in Figures 6, and 7 are best viewed zoomed in.

3. Simulated anomaly training of state-of-the-art supervised methods

We trained the recent supervised anomaly detection methods [3, 5] on the MVTec [1] dataset using the synthetic anomalies generated by the proposed anomaly simulation method. The results are listed in Table 1. DRÆM outperforms both evaluated methods by a large margin, indicating that besides generating synthetic labels, also the entire architecture combining reconstructive and discriminative sub-architectures is needed to achieve best results.

Methods	Detection	Localization
DRÆM	**98.0**	**97.3**
Rački *et al*. [5]	90.7	84.3
Božič *et al*. [3]	92.8	93.9

Table 1: Anomaly detection and localization performance of supervised methods [3, 5] trained using simulated anomalies on the MVTec dataset [1]. Results are listed in AUROC and pixel-based AUROC for detection and localization, respectively.

References

[1] Paul Bergmann, Michael Fauser, David Sattlegger, and Carsten Steger. MVTec AD – A Comprehensive Real-World Dataset for Unsupervised Anomaly Detection. In *Proceedings of the IEEE Conference on Computer Vision and Pattern Recognition*, pages 9592–9600, 2019. 1, 2, 3, 4, 5

[2] Paul Bergmann, Michael Fauser, David Sattlegger, and Carsten Steger. Uninformed students: Student-teacher anomaly detection with discriminative latent embeddings. In *Proceedings of the IEEE/CVF Conference on Computer Vision and Pattern Recognition*, pages 4183–4192, 2020. 1, 5

[3] Jakob Božič, Domen Tabernik, and Danijel Skočaj. End-to-end training of a two-stage neural network for defect detection. *25th International Conference on Pattern Recognition ICPR*, 2020. 1, 7, 8

[4] Thomas Defard, Aleksandr Setkov, Angelique Loesch, and Romaric Audigier. Padim: a patch distribution modeling framework for anomaly detection and localization. In *1st International Workshop on Industrial Machine Learning, ICPR 2020*, 2020. 5

[5] D. Rački, D. Tomaževič, and D. Skočaj. A compact convolutional neural network for textured surface anomaly detection. In *2018 IEEE Winter Conference on Applications of Computer Vision (WACV)*, pages 1331–1339, 2018. 1

[6] M Wieler and T Hahn. Weakly supervised learning for industrial optical inspection, 2007. 1, 7, 8

[7] Vitjan Zavrtanik, Matej Kristan, and Skočaj Danijel. Reconstruction by inpainting for visual anomaly detection. *Pattern Recognition*, 2020. 1, 5

(a) Capsule

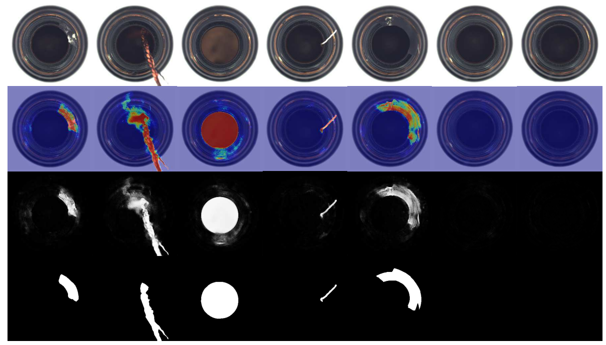

(b) Bottle

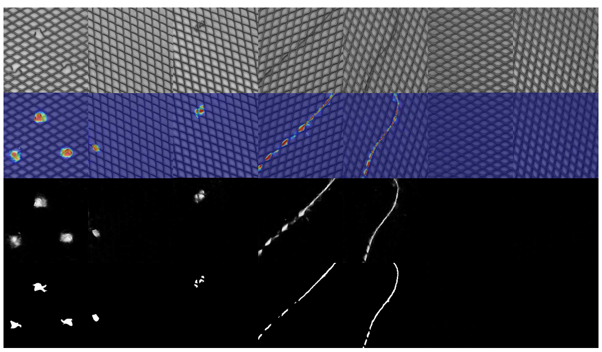

(c) Grid

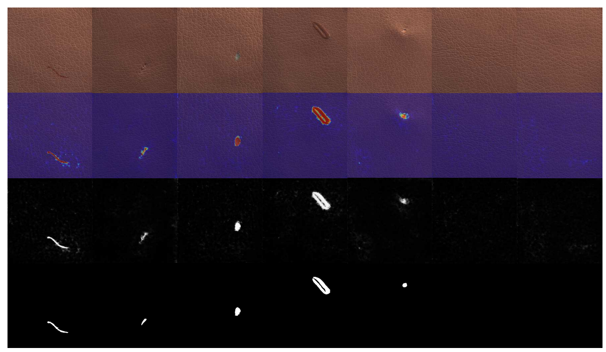

(d) Leather

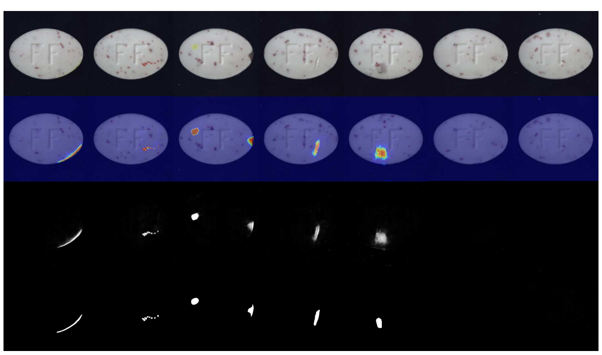

(e) Pill

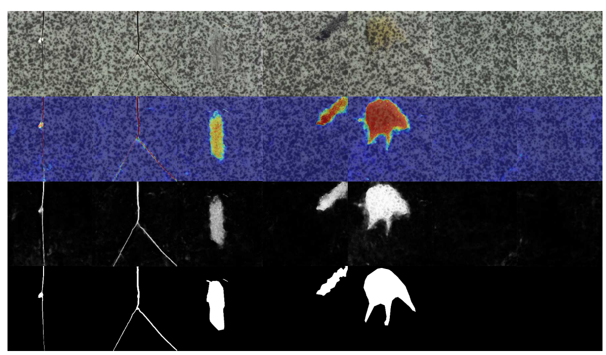

(f) Tile

Figure 1: DRÆM qualitative examples for the MVTec dataset [1]. The original image, the anomaly overlay, the output anomaly map and the ground truth map are shown. Best viewed zoomed in.

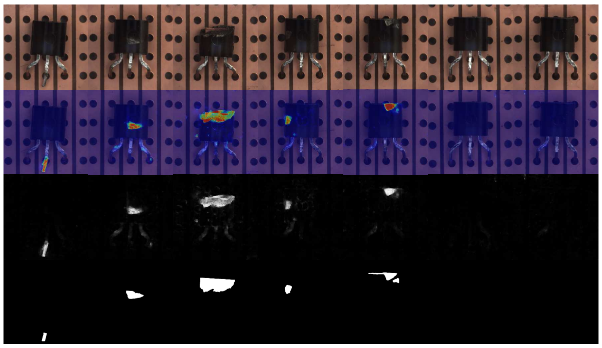

(a) Transistor

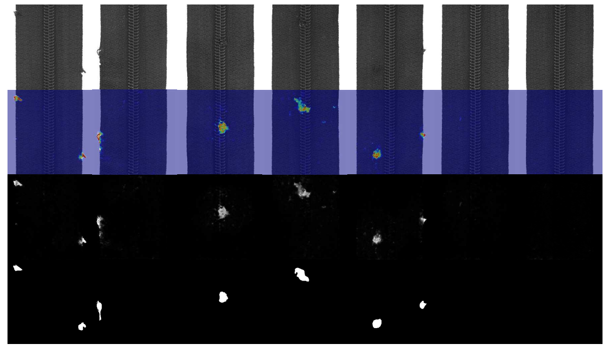

(b) Zipper

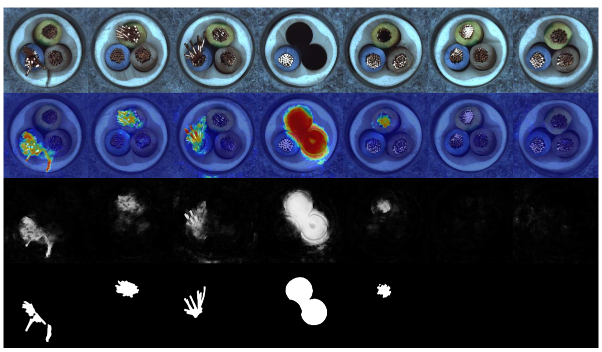

(c) Cable

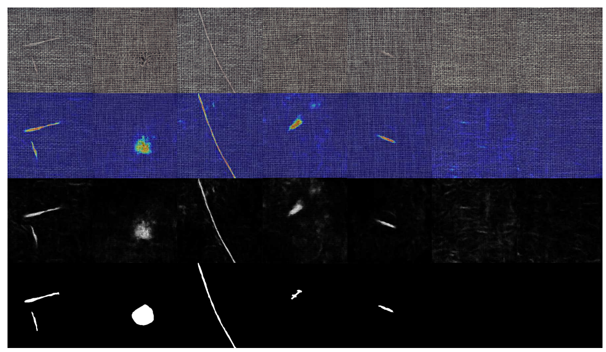

(d) Carpet

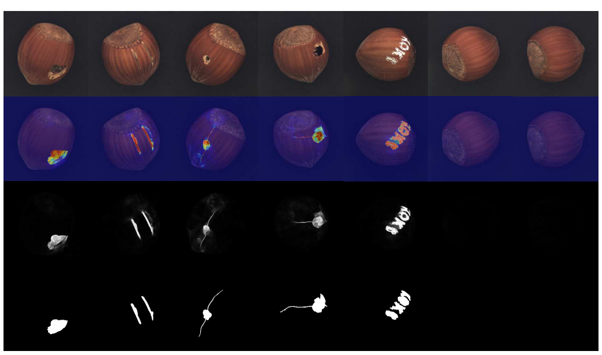

(e) Hazelnut

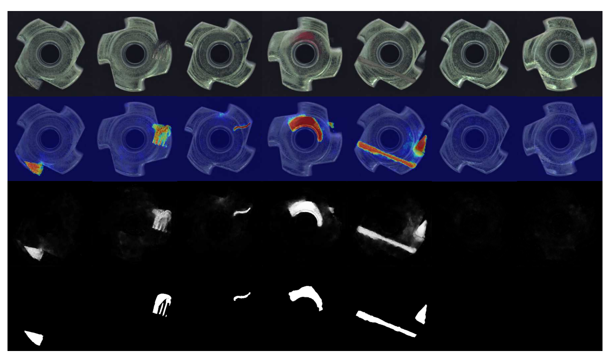

(f) Metal nut

Figure 2: DRÆM qualitative examples for the MVTec dataset [1]. The original image, the anomaly overlay, the output anomaly map and the ground truth map are shown.

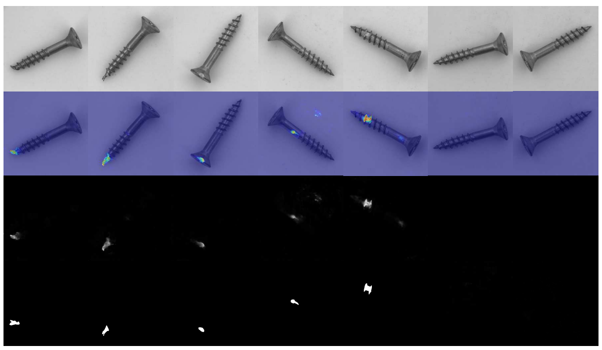

(a) Screw

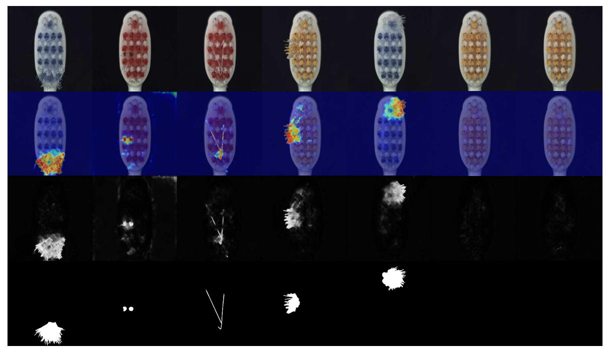

(b) Toothbrush

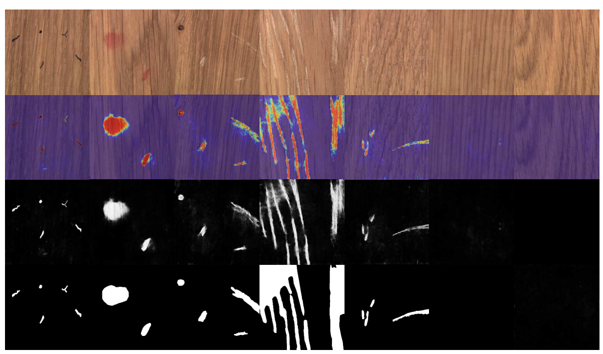

(c) Wood

Figure 3: DRÆM qualitative examples for the MVTec dataset [1]. The original image, the anomaly overlay, the output anomaly map and the ground truth map are shown.

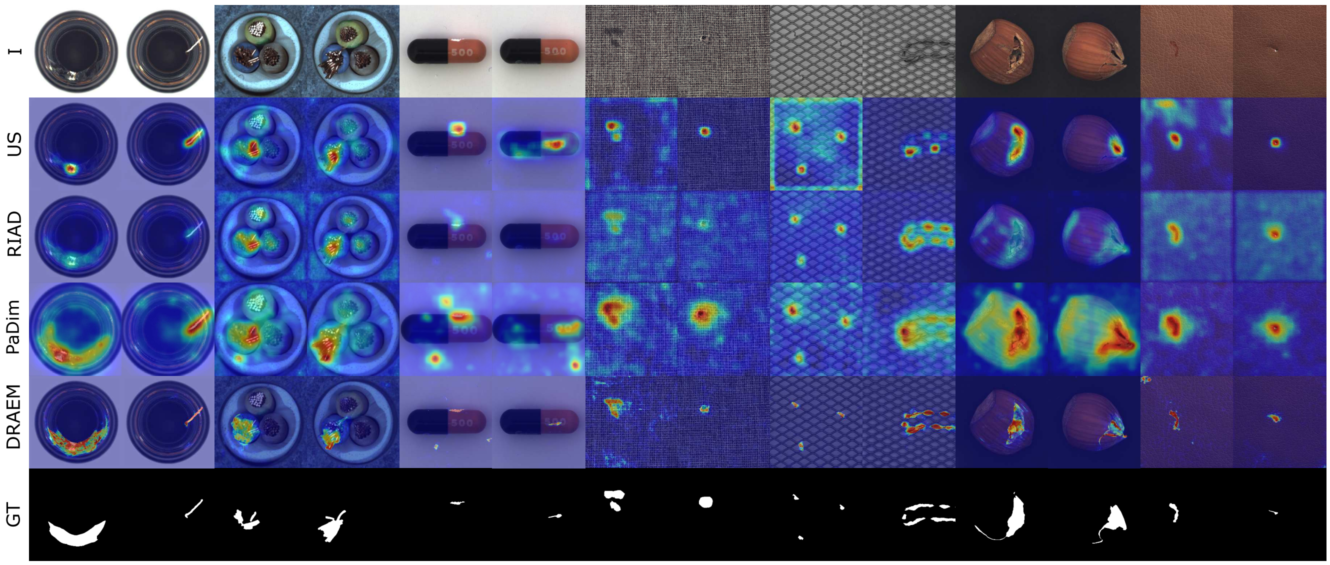

(a)

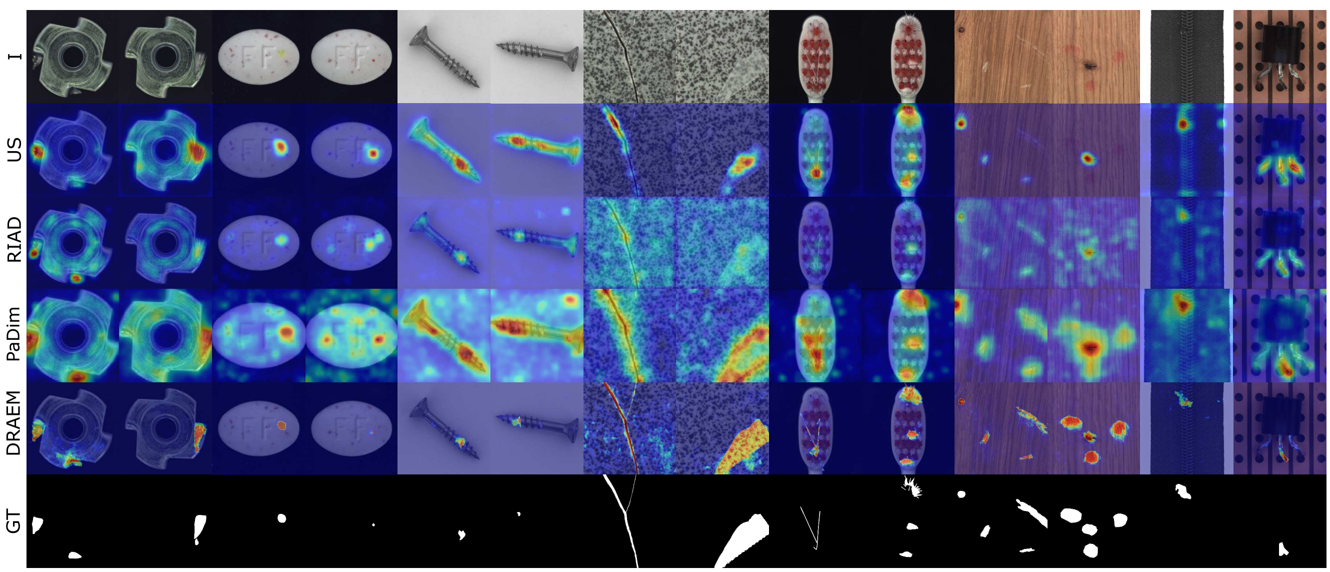

(b)

Figure 4: Qualitative comparison of DRÆM to the recent anomaly detection methods US [2], RIAD [7] and PaDim [4] on the MVTec dataset [1]. The original image (I), the anomaly overlays for all methods and the ground truth map (GT) are shown.

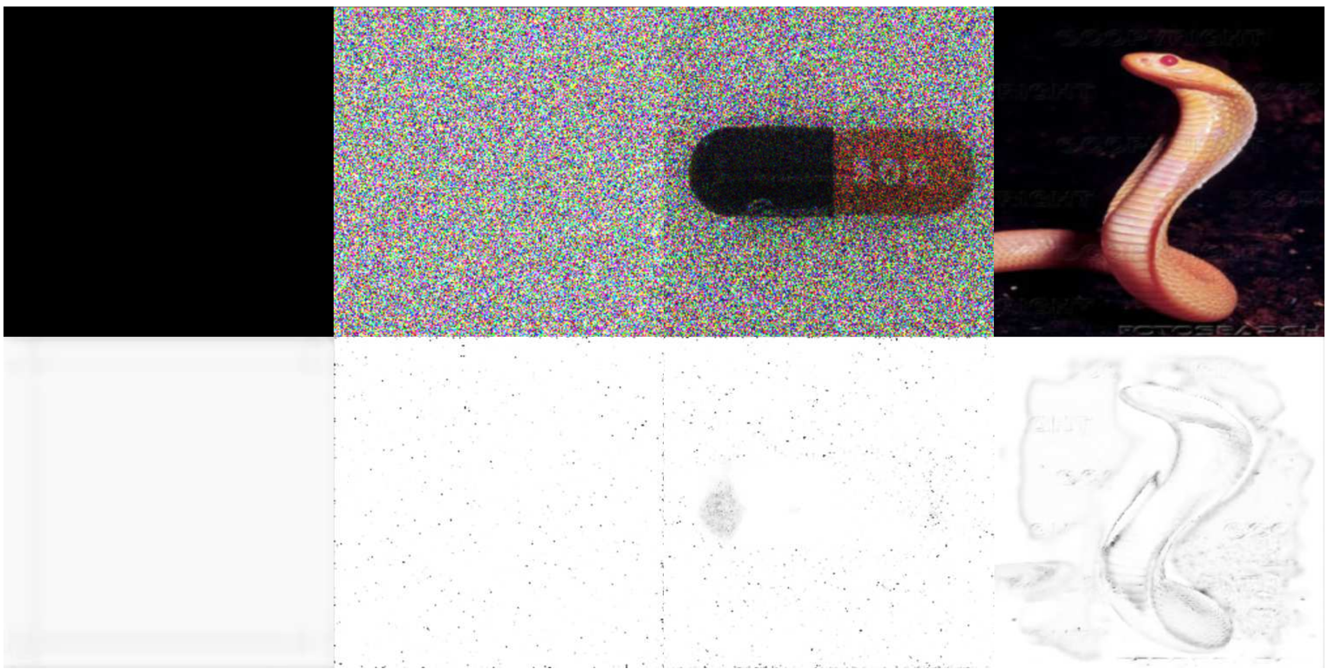

Figure 5: The output anomaly maps on entirely anomalous images. The input image and the output of DRÆM are shown in the first and second row, respectively. An image filled with zeros, a uniform noise image, an anomaly-free image with added uniform noise and a completely out-of-distribution image are shown from left to right. DRÆM correctly marks the vast majority of pixels as anomalous.

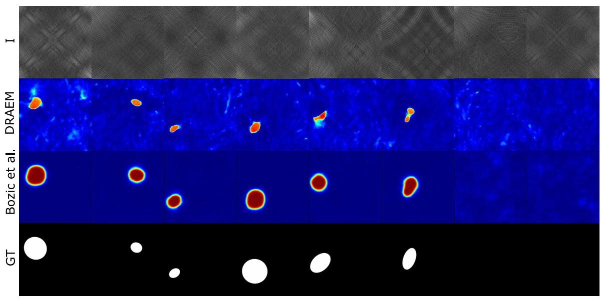

(a) Class1

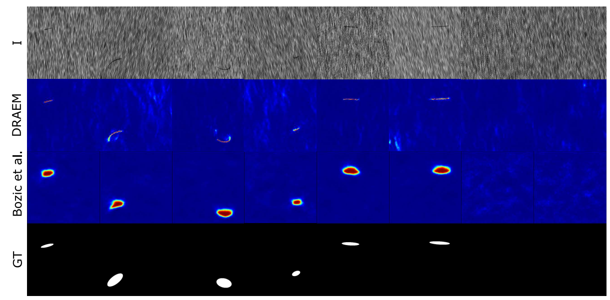

(b) Class2

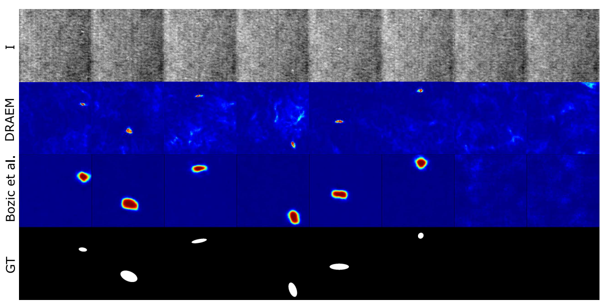

(c) Class3

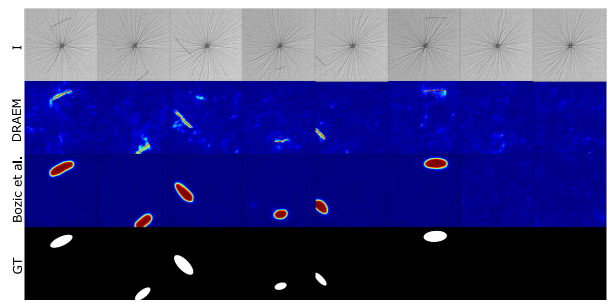

(d) Class4

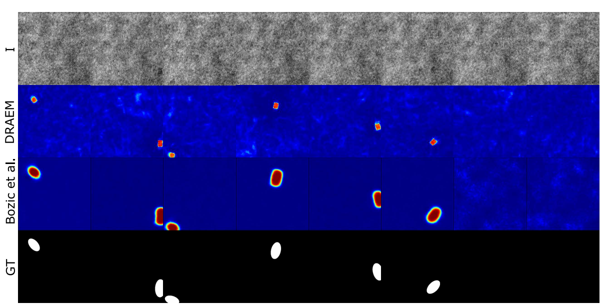

(e) Class5

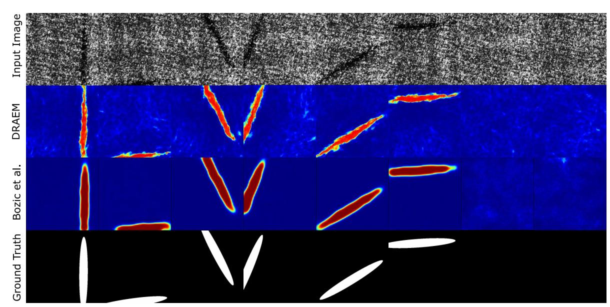

(f) Class6

Figure 6: Qualitative examples for the DAGM dataset [6]. The original image I, the DRÆM anomaly map, the anomaly map produced by Bozic *et al*. [3] and the ground truth map GT are shown.

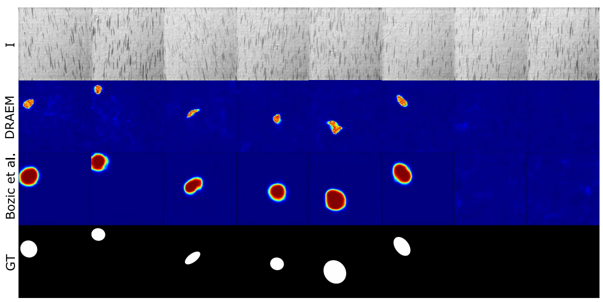

(a) Class7

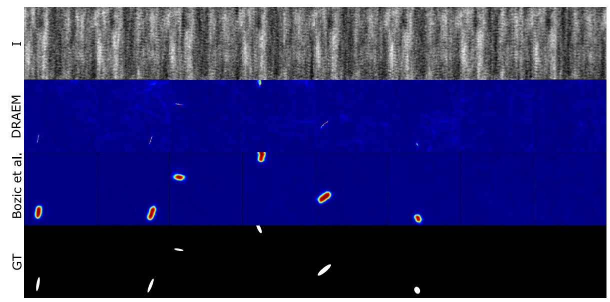

(b) Class8

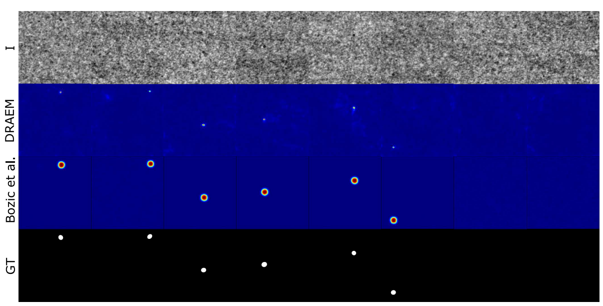

(c) Class9

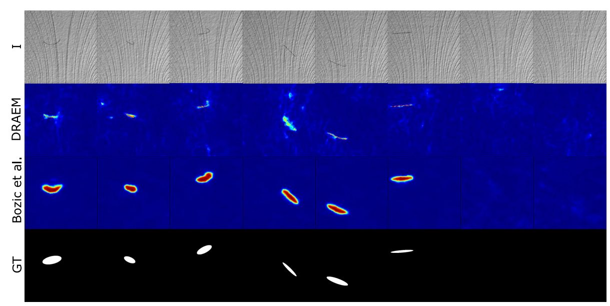

(d) Class10

Figure 7: Qualitative examples for the DAGM dataset [6]. The original image (I), the DRÆM anomaly map, the anomaly map produced by Bozic *et al*. [3] and the ground truth map (GT) are shown.